Environmental Science & Technology

pubs.acs.org/est

Article

The Coupled Effect of Light and Iron on the Photogranulation Phenomenon

Abeera A. Ansari, Arfa A. Ansari, Joseph G. Gikonyo, Ahmed S. Abouhend, and Chul Park*

Cite This: *Environ. Sci. Technol.* 2023, 57, 9086−9095

Read Online

ACCESS | Metrics & More | Article Recommendations | Supporting Information

ABSTRACT: Cyanobacteria occasionally self-immobilize and form spherical aggregates. This photogranulation phenomenon is central for oxygenic photogranules, which present potential for aeration-free and net-autotrophic wastewater treatment. Light and iron are tightly coupled via photochemical cycling of Fe, suggesting that phototrophic systems continually respond to their combined effects. Thus far, photogranulation has not been investigated from this important aspect. Here, we studied the effects of light intensity on the fate of Fe and their combined effects on the photogranulation process. Photogranules were batch-cultivated with the activated sludge inoculum under three photosynthetic photon flux densities: 27, 180, and 450 μmol/m^2·s. Photogranules were formed within a week under 450 μmol/m^2·s compared to 2−3 and 4−5 weeks under 180 and 27 μmol/m^2·s, respectively. Batches under 450 μmol/m^2·s showed faster but lower quantity of Fe(II) release into bulk liquids compared to the other two sets. However, when ferrozine was added, this set showed substantially more Fe(II), indicating that Fe(II) released by photoreduction undergoes fast turnover. Fe linked with extracellular polymeric substances (EPS), Fe_{EPS}, diminished significantly faster under 450 μmol/m^2·s, while the granular shape in all three batches appeared along with the depletion of this Fe_{EPS} pool. We conclude that light intensity has a major influence on the availability of Fe, and light and Fe together impact the speed and characteristics of photogranulation.

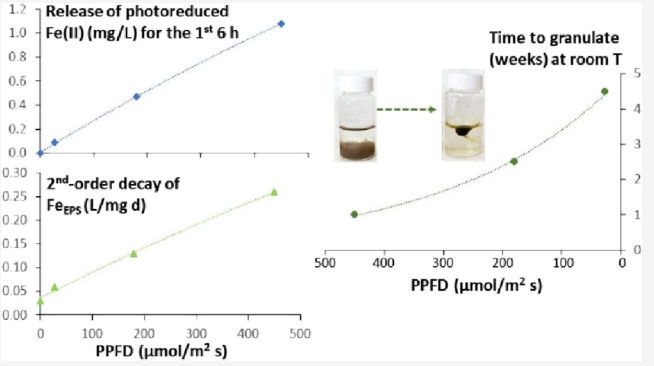

KEYWORDS: *photogranulation, light, iron, photochemical reduction, cyanobacteria, EPS*

INTRODUCTION

Phototrophic organisms capture light via a photosynthetic apparatus, which has strong coupling with iron.[1] The photosynthetic electron transport chain possesses many Fe-containing molecules, including cytochrome c, cytochrome b6f, Fe-S protein, and ferredoxin.[2,3] Furthermore, Fe is present within the reaction centers of both photosystems I and II and is involved in the biosynthesis of photopigments.[4,5] More than 50% of metabolic Fe resides in the photosynthetic apparatus,[4,6] which demonstrates the codependence of the phototrophic community on light and Fe for metabolism. The dual limitation of Fe and light availability will, hence, repress phototrophic growth, whereas dual enrichment of light and Fe availability will promote phototrophic bloom.[1,7]

Photochemical cycling of Fe is another crucial aspect of the coupling of light and Fe and its impact on microbial growth in the ecosystem. In the photochemical reduction process, Fe(III) complexed with photolabile organic ligands, such as polycarboxylate molecules, is reduced and released as unchelated Fe(II), once an electron is transferred from the ligand to the metal center under irradiation, i.e., the ligand-to-metal charge transfer reaction.[8−10] This photogenerated Fe(II) is considered the most available form of Fe for phototrophs, which has been supported by significantly increased biological Fe uptake.[8,11] Similarly, cyanobacterial uptake of Fe directly increased in correspondence to the increase in levels of photoproduced unchelated Fe(II) from the original Fe(III)-EDTA complex.[10] Interestingly, the same study showed that in the spectrum of visible light, it was primarily the 400−500 nm wavelength that caused both photochemical reduction of Fe and its uptake by cyanobacteria.

Cyanobacteria are known to have a high Fe requirement compared to other phototrophs and heterotrophic bacteria[12,13] and thus have strong physiology codependence on light and Fe availability.[14] Cyanobacteria occasionally granulate, forming a sphere-like aggregate. The occurrence of this photogranulation phenomenon has been reported from various natural environments, including sea,[15,16] lakes,[17,18] and even extreme environments like glaciers.[19−22] For the latter, a photogranular product

Received: January 16, 2023
Revised: May 25, 2023
Accepted: May 26, 2023
Published: June 5, 2023

https://doi.org/10.1021/acs.est.3c00432
Environ. Sci. Technol. 2023, 57, 9086−9095

cryoconite occurs on surfaces of glaciers around the globe and has been linked with the expansion of surface darkening and enhanced glacial melt.[19,23] The cyanobacteria-based photogranulation has also been the basis for the production of oxygenic photogranules (OPGs) in built systems.[24−30] OPGs present potential to treat wastewater without aeration, which currently requires the highest level of energy in wastewater treatment, and to accomplish the net autotrophy of wastewater treatment.[29,31] The seed OPG biomass can be produced by batch incubation of activated sludge under both hydrostatic[24,32−34] and hydrodynamic[35] conditions with an illumination source. The former typically employs small (∼20 mL) closed glass vials, while the latter has used 1 L glass jars open to the atmosphere.

The importance of Fe in photogranule systems has been recently documented.[32,36,37] In a closed hydrostatic batch with the activated sludge inoculum under a photosynthetic photon flux density (PPFD) of 18−45 μmol/m^2·s, the availability of Fe, the growth of cyanobacteria, and the appearance of granular structure correlated.[32] In this batch, a quick and significant increase of bulk-liquid Fe—both Fe(II) and Fe(III)—first occurred, presumably due to photochemical reduction of Fe under illumination, initial anaerobic condition development in closed vials, and subsequent dissociation of the sludge biomass. During this early batch period, growth of eukaryotic microalgae was also vivid, indicating the availability of this bulk-liquid Fe for their growth. This microalgal growth and reoxygenation of the batch system led to depletion of bulk-liquid Fe. Then, significant growth of filamentous cyanobacteria, particularly the order Oscillatoriales, was observed. Importantly, this cyanobacterial bloom coincided with a substantial decrease of Fe that is bound with extracellular polymeric substances (EPS) in inocula, Fe_{EPS}, suggesting the Oscillatoriales' ability to access and utilize activated sludge EPS for the source of Fe. The study further pointed out that a spherical structure ensued with depletion of this Fe_{EPS} pool, suggesting that the availability of Fe has a significant impact on cyanobacterial physiology and granulation.

Despite the important roles that Fe and light play in cyanobacterial growth and physiology, the effect of light conditions on the fate and availability of Fe and their coupled effects on the photogranulation phenomenon remain unexplored and hence unknown. Here, we studied how different light intensities impact dynamics of bulk-liquid Fe and the fate of Fe_{EPS} and how they are related to the progression of the photogranulation process. We also studied the extent of photochemical reduction of Fe under different light intensities by incubating activated sludge with ferrozine, a strong Fe(II) chelator. We chose the hydrostatic batch system for this study for its advantage in controlling experiments and tracking changes that occur during batch reactions. The strong resemblance of photogranulation phenomena occurring in different batch settings and flow-through reactors as well as their photogranular products is well-discussed in the literature.[24,31,34−36,38,39] This study is expected to further the knowledge of the photogranulation phenomenon, helping to develop OPGs for aeration-free and net-autotrophic wastewater treatment and better understand other photogranular products that occur in varying natural environments on our biosphere.

MATERIALS AND METHODS

Hydrostatic Batch Cultivation Setup. Each 20 mL glass vial was inoculated with 10 mL of activated sludge, collected from the aeration basin of a local wastewater treatment plant (Amherst, MA), and sealed with sterile caps. These vials were left unmixed under three PPFD: 27 ± 9, 180 ± 36, and 450 ± 56 μmol/m^2·s. LED panels with full-spectrum white light were used to provide continuous illumination. The vials placed under dark conditions served as a dark control. All cultivations were conducted inside a 22 °C temperature-controlled room.

Fate and Dynamics of Fe. Over the batch period, the concentrations of Fe in bulk liquid (0.45 μm filtrate of samples), biomass-bound EPS, and whole biomass were measured, which allowed us to track their changes and conduct mass balance on Fe.[32,36] For Fe in bulk liquid, we considered two fractions: dissolved Fe (<30 kDa) and colloidal Fe (30 kDa—0.45 μm). Filtrations were conducted in a glovebox under continuous N_2 purging, and filtrates were quickly acidified with trace-metal grade HNO_3. The total Fe concentration in bulk-liquid filtrates was measured by inductively coupled plasma-mass spectrometry (ICP-MS, PerkinElmer SCIEX). The Fe(II) concentration in the same filtrates was measured by the ferrozine reagent method.[40] The concentration of Fe(III) was then obtained by subtracting Fe(II) from total Fe. For Fe in the extractable EPS fraction (Fe_{EPS}), EPS of biomass was first extracted employing sequential sonication and base treatment.[32,41] Both EPS extracts were acidified with HNO_3 prior to the analysis of Fe by ICP-MS. Fe_{EPS} was the summation of Fe present in the sonication-extracted EPS (1st step) and the base-extracted EPS (2nd step). Fe in the whole biomass was determined using the standard methods (3030E),[42] which involves acid digestion of the whole biomass and analysis with ICP-MS.

Photochemical Fe Reduction Potential. Additional batches were prepared containing 10 mL of activated sludge (AS) spiked with a 200 μM ferrozine (FZ) reagent. These vials were then placed under three light conditions and dark conditions described above. FZ is a strong Fe(II) chelator, which forms an $Fe^{II}FZ_3$ complex in the first-order reaction.[10] Furthermore, the $Fe^{II}FZ_3$ complex is not bioavailable as FZ does not cross the plasma membrane.[43,44] Therefore, it would be reasonable to assume that the rate of $Fe^{II}FZ_3$ formation is the rate of Fe(II) release from the AS inoculum. Additionally, we attempted to estimate the extent of Fe(II) release due to photochemical reduction using the following equation:

$$\text{Fe(II) release due to photoreduction} = \text{Fe(II) in (AS + FZ)}_{\text{Light}} - \text{Fe(II) in (AS + FZ)}_{\text{Dark}} \quad (1)$$

Fe(II) concentrations were obtained by first measuring $Fe^{II}FZ_3$ absorbance of 0.45 μm bulk liquid at 562 nm and by quantifying per the ferrous ammonium sulfate standard with FZ. We also determined total Fe concentrations in the same bulk liquids of AS+FZ (both light and dark) via ICP-MS.

Analytical Measurements. Total solids, volatile solids, and chlorophyll contents of samples were determined using the standard methods.[42] The phycobiliprotein concentration was determined following Bennett and Bogorad[45] with modification,[32] which involves removing background interferences from absorbances.[46] The polysaccharide concentration in bulk liquids and EPS was measured using the phenol-sulfuric method with glucose as a standard.[47] For measurements of the

https://doi.org/10.1021/acs.est.3c00432
Environ. Sci. Technol. 2023, 57, 9086−9095

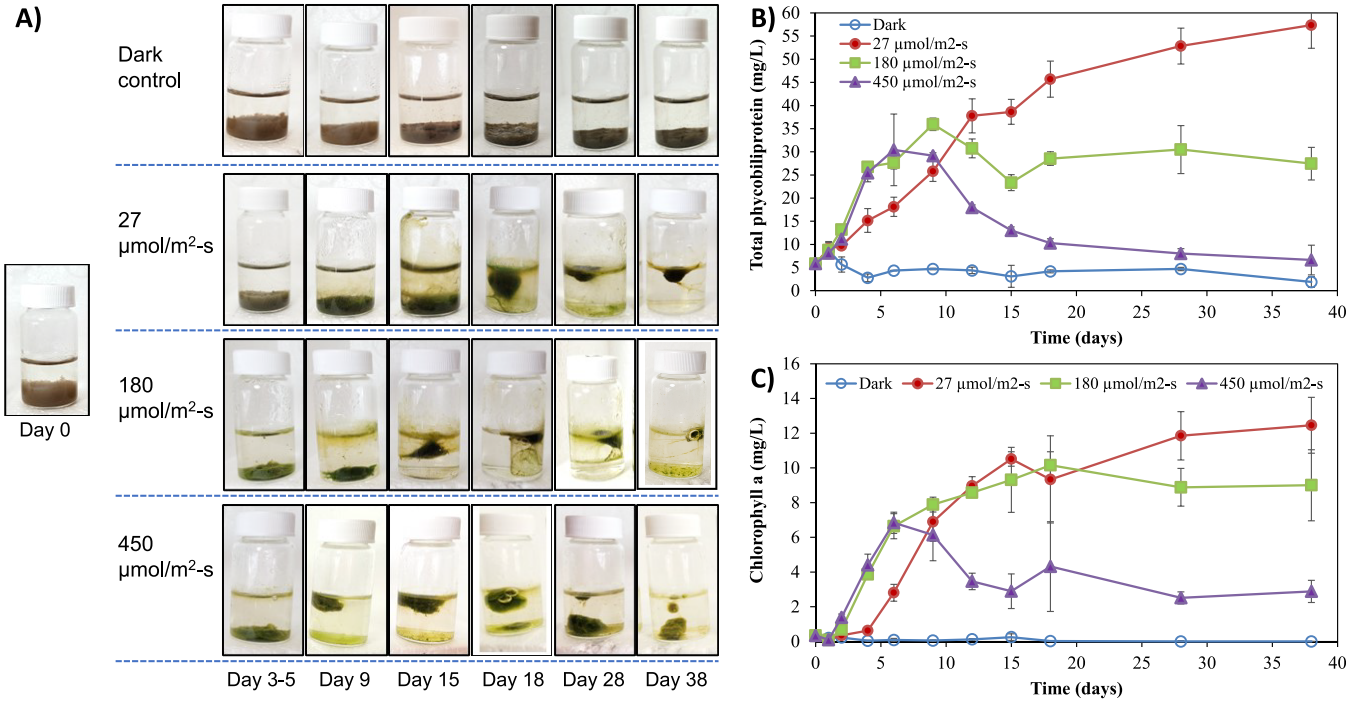

Figure 1. Progression of photogranulation with the activated sludge inoculum in a hydrostatic environment under different light intensities. (A) Photos of batches on different days under no light (dark control), 27, 180, and 450 μmol/m^2·s. (B) Growth of cyanobacteria indicated with the concentration of total phycobiliprotein. (C) Growth of oxygenic phototrophs indicated with the concentration of chlorophyll *a*. Error bars represent standard deviation from triplicate batch samples.

concentrations of protein and humic substances, we used the Frølund adaptation[48] of the Lowry method[49] with bovine serum albumin as a standard. Dissolved oxygen (DO) in batches was monitored using a portable DO probe inside the glovebox with continuous N_2 purging.

Microscopy. Light and autofluorescence microscopy (EVOS FL Color, AMEFC4300) was frequently employed over the batch period. For formed photogranules, we also conducted microscopy on the outer and inner sections of photogranular samples. For this, photogranules were frozen at −20 °C prior to cross-sectioning. The frozen photogranules were placed on wax sheets and cut off at various sections with a sterile razor blade. The presence of filamentous cyanobacteria was confirmed via RFP excitation (530 nm), which produced golden-orange fluorescence for a phycobilin pigment phycoerythrin in cyanobacteria.[50]

Statistical Analysis. The Pearson correlation coefficient (r) was determined among variables, and the two-sample t-test (α = 0.05) analysis was conducted to evaluate the statistical significance between variables.

RESULTS AND DISCUSSION

Impact of Light Intensity on Progression of Photogranulation. Light intensity influenced the speed of photogranulation (Figure 1A). Under 27 μmol/m^2·s, significant contraction and floating of biomass took place between days 15 and 18 followed by granular structures appearing on around day 28. Progression of granulation in 180 and 450 μmol/m^2·s was faster. Under 180 μmol/m^2·s, granules were seen on around day 15, while under 450 μmol/m^2·s, mature granules already appeared before day 9. Unlike lower lighting sets, however, continued batch under 450 μmol/m^2·s resulted in the loosened granular structure, accompanied by the loss of cyanobacterial layers (Figure S1). These observations suggest that there is a threshold light intensity above which formed photogranules become dissociated if the batch period is prolonged.

Microscopy revealed dominant phototrophic communities over the cultivation period and their spatial distribution in the formed granular biomass (Figure S2). Under 27 μmol/m^2·s, significant cyanobacterial growth occurred along with the development of a peelable cyanobacterial outer layer. In this set, Oscillatoriales were observed to migrate outward in granules, probably to harness more light. The 180 μmol/m^2·s set, in contrast, showed the bloom of microalgae before the abundant growth of Oscillatoriales. These cyanobacteria eventually enveloped the microalgae and other biomass into a granule, with only a few cyanobacteria trichomes remaining in the center of granules. The 450 μmol/m^2·s batch showed a significant growth of microalgae during week 1, but cyanobacteria also grew fast during the same period, coinciding with fast formation of photogranules (Figure 1A). In this set, Oscillatoriales were seen to migrate inward, possibly to avoid photoinhibition.[51−54] Consequently, more trichomes were located toward inner parts of photogranules, and outer parts exhibited a lower cyanobacterial population than those from lower light sets (Figure S2). In the 450 μmol/m^2·s batch, again, the cyanobacterial population diminished over continued incubation, which occurred with diminished granular integrity (Figure S1 and Figure 1A).

The results of photosynthetic pigments concurred with macroscopic and microscopic observations. The batch under 27 μmol/m^2·s led to the production of phycobilin up to 57 ± 5 mg/L, much greater than that under 180 and 450 μmol/m^2·s (Figure 1B). Cyanobacteria have phycobilin, an additional light-harvesting pigment. Furthermore, cyanobacteria have a lower maintenance requirement than microalgae under light-

https://doi.org/10.1021/acs.est.3c00432
Environ. Sci. Technol. 2023, 57, 9086−9095

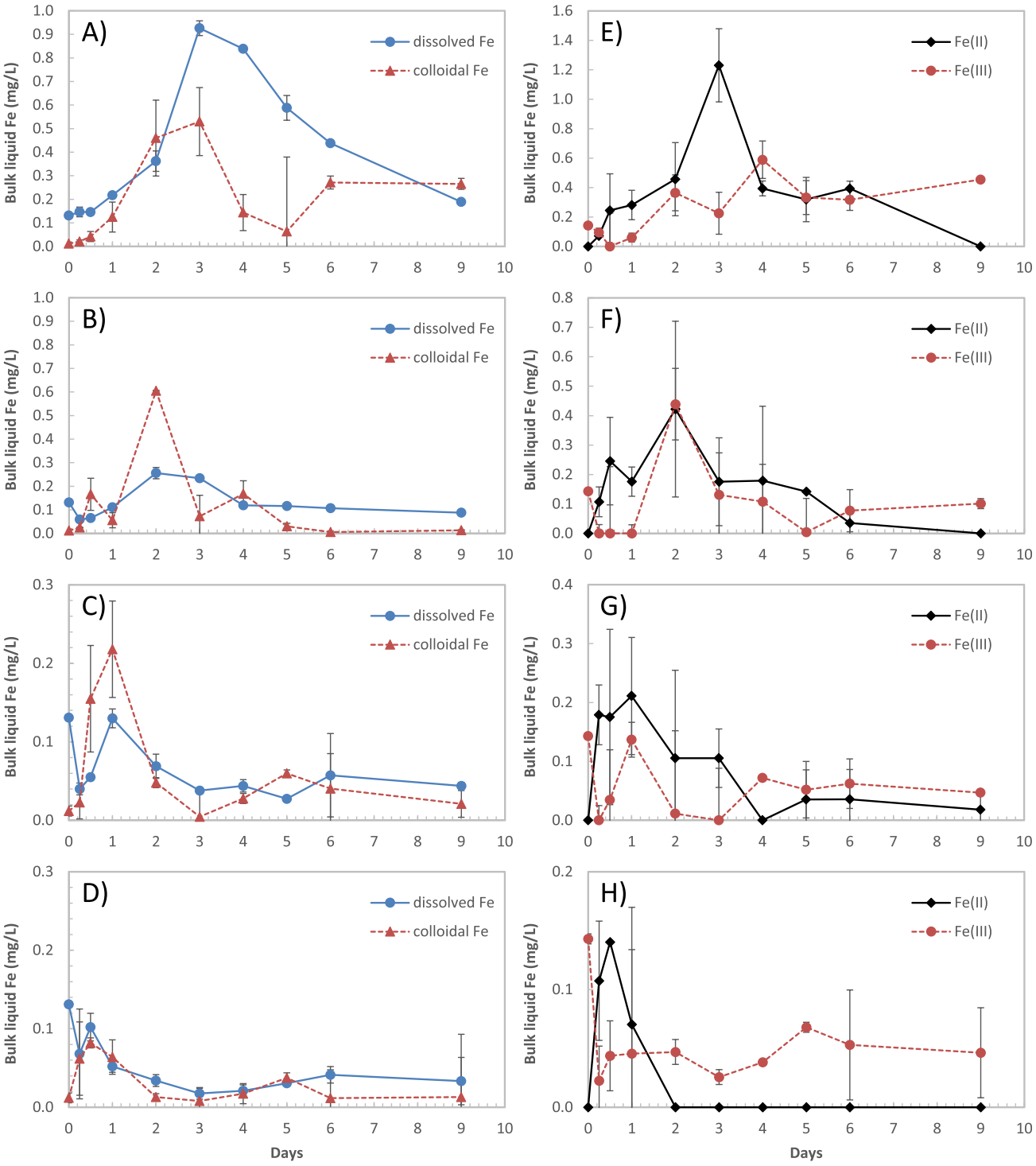

Figure 2. Changes in quantities and characteristics of Fe in bulk liquids of batches for the first 9 days: dark control (A,E), 27 (B,F), 180 (C,G), and 450 μmol/m^2·s (D,H). (A−D) Dissolved (<30 kDa) and colloidal (30 kDa—0.45 μm) Fe in bulk liquids. (E−H) Fe(II) and Fe(III) in bulk liquids. The results for the entire batch period (38 days) are shown in the Supporting Information (Figure S3). Note different scales used in each figure. Error bars represent standard deviation from triplicate cultivation samples.

limited conditions.[53] These suggest that a low light intensity of 27 μmol/m^2·s posed a selection pressure toward cyanobacteria. In the 180 μmol/m^2·s set, the phycobilin concentration increased till day 9 and remained relatively constant afterward. In the 450 μmol/m^2·s batch, the peak phycobilin concentration was observed by week 1, but it quickly declined later, indicating a significant loss of the cyanobacterial population. The results of chlorophyll *a* exhibited a similar trend to phycobilin (Figure 1C), supported by positive correlations between chlorophyll *a* and phycobilin: most strongly under 27 μmol/m^2·s (r = 0.97) followed by 180 (r = 0.86) and 450 μmol/m^2·s (r = 0.85).

Influence of Light Intensity on Dynamic Changes of Fe in Bulk Liquid. The bulk-liquid Fe concentration in the activated sludge inoculum was, on average, 0.14 mg/L, accounting for 0.7% of total Fe (21.5 mg/L) in the inoculum.

https://doi.org/10.1021/acs.est.3c00432
Environ. Sci. Technol. 2023, 57, 9086−9095

Its majority (>90%) was present in the dissolved fraction (<30 kDa) (Figure 2A−D and Figure S3), while Fe(II) was undetected (Figure 2E−H and Figure S3). As the batch incubation proceeded, Fe(III) in bulk liquids became quickly depleted, which corresponded with the rapid appearance of Fe(II) (Figure 2E−H). This phenomenon was prominent under illumination because it happened within the first sampling point (6 h) of all light batch sets, implying photochemical reduction of Fe(III). Furthermore, DO in the light sets got depleted significantly faster than in the dark control (Figure S4), indicating enhanced biotic and abiotic reactions under illumination. This early depletion of DO might have also facilitated reduction of Fe. The DO in batches under 450 and 180 μmol/m^2·s then rapidly bounced back as photosynthesis became prevalent.

As more Fe(II) was found in bulk liquids, indicating reduction and release of Fe from the solid-phase inoculum,[32] Fe(III) also reappeared in bulk liquids, and both Fe(II) and Fe(III) soon reached their peak. It is very likely that the bulk-liquid Fe(III) in the lighting sets resulted from the reoxidation of Fe(II) due to reoxygenation by oxygenic photosynthesis (Figure S4). In this regard, it is worth noting that when the peak release happened, the ratio of Fe(II) to Fe(III) in bulk liquids increased with the light intensity, implying a greater photochemical reduction pressure under higher light intensities and co-occurrence of reduction and reoxidation of Fe. Meanwhile, the reappearance of Fe(III) in the dark control could have been due to reoxidation of Fe(II) by nitrate-dependent anaerobic Fe(II) oxidizing bacteria,[55] which produces Fe(III) and denitrification products under anoxic, circumneutral pH conditions.[56] After these peak points, Fe(II) was rapidly removed from bulk liquids. Under 450 μmol/m^2·s, Fe(II) was undetected from day 2. Under 180 μmol/m^2·s, Fe(II) was undetected or found at extremely low levels from day 4. Fe(II) lingered longer in the 27 μmol/m^2·s batch and dark control but was also undetected from day 9. Small amounts of Fe(III) persisted in bulk liquids of all light sets. There, Fe(III) of <0.1 mg/L was consistently found, and the majority of this Fe was in the dissolved fraction, similar to the activated sludge inoculum. These suggest that in oxic aqueous environments, a small amount of Fe(III) exists as dissolved complexes, likely complexes of Fe(III)-organic ligands.[57]

The times for peak for both Fe(II) (Figure 2E−H and Figure S3) and bulk-liquid Fe (Figure 2A−D and Figure S3) and their declination speeds suggest that light intensity has a significant impact on photochemical reduction of Fe and subsequent reactions. The peak times under 450, 180, and 27 μmol/m^2·s and no light were 0.5, 1, 2, and 3 days, respectively. The peak concentration values, however, showed the opposite trend, i.e., the lowest for 450 μmol/m^2·s and the highest for the dark control. These results imply faster photoreduction and release of Fe as well as assimilation of bulk-liquid Fe under higher light conditions. These points are corroborated by faster growth of phototrophic microbes under stronger illuminations (Figure 1B,C) and negative correlations between bulk-liquid Fe and photosynthetic pigments in all light batches. The correlation coefficient r for dissolved Fe vs phycobilin was −0.80, −0.89, and −0.57 for 27, 180, and 450 μmol/m^2·s, respectively. The coefficients with chlorophyll a were, respectively, −0.81, −0.78, and −0.53.

All the above results suggest that early dynamic changes of bulk-liquid Fe in hydrostatic batches under illumination have significant association with photoreduction of Fe. Furthermore, the measured bulk-liquid Fe is only the net result of varying reactions, including assimilation of the released Fe by phototrophic communities.

Extent of Photochemical Reduction of Fe under Different Light Intensities. To gain better insight into the impact of light intensity on photoreduction of Fe and further effects on photogranulation, we also conducted batches with ferrozine addition (+FZ). All +FZ batches, including the dark control, showed the formation of $Fe^{II}FZ_3$, shown by the development of magenta color in bulk liquids, indicating the release of unchelated Fe(II) into bulk liquids during hydrostatic batches of activated sludge. Quantification of Fe(II), via measurements of $Fe^{II}FZ_3$, in +FZ sets further revealed important information. Most notably, levels of Fe(II) in bulk liquids of +FZ batches (Figure 3A) were substantially

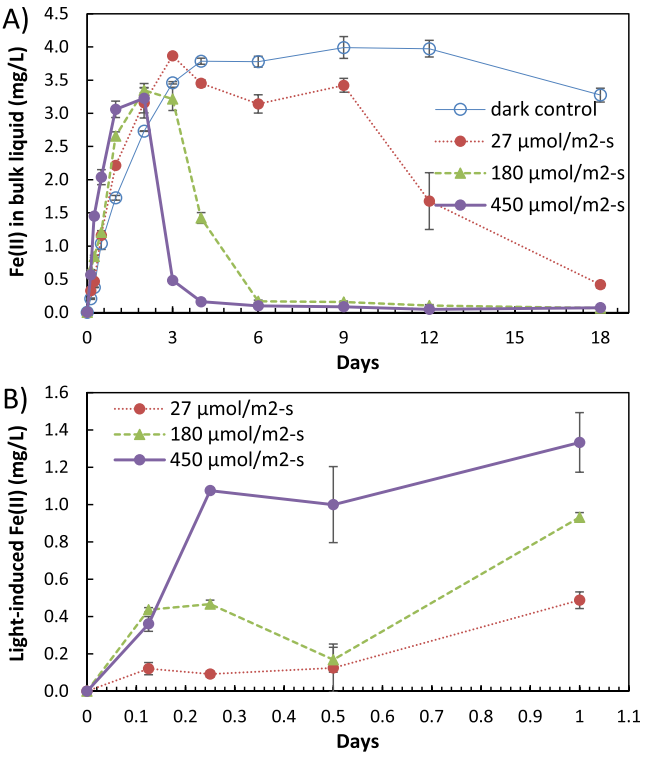

Figure 3. Release of Fe(II) into bulk liquids of batches with the addition of ferrozine (+FZ). (A) Fe(II) concentration in bulk liquids. (B) Light-induced Fe(II) release, which was obtained by subtracting Fe(II) + FZ of the dark control from Fe(II) + FZ of batches under different light intensities. Error bars represent standard errors from duplicate batch samples.

greater than both bulk-liquid Fe(II) and Fe(III) in batches without FZ (Figure 2); measurements of the bulk-liquid Fe in +FZ batches by ICP-MS also confirmed this (data not shown). These results suggest that the extent of Fe(II) release in batches without FZ should have been significantly greater than the measured values (Figure 2). Consequently, this would also mean that the released unchelated Fe(II) in batches was quickly removed from the bulk-liquid phase.

Comparing the results among three light sets as well as with the dark control reveals that light intensity has a significant influence on photochemical reduction and release of Fe(II) into bulk liquids. First of all, the release of Fe(II) in the dark control, which by the way was slower than any light sets (Figure 3A), reflects reduction and release of Fe(II) by

https://doi.org/10.1021/acs.est.3c00432
Environ. Sci. Technol. 2023, 57, 9086−9095

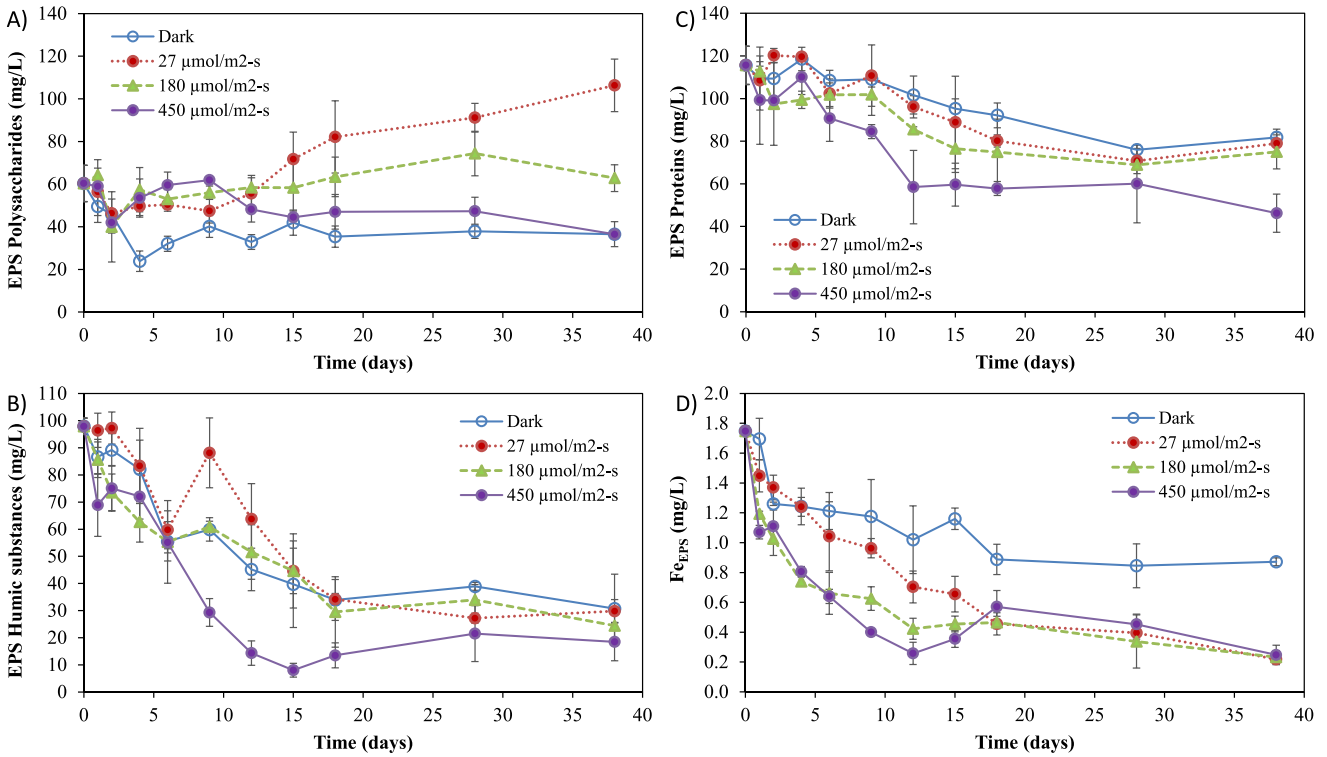

Figure 4. Changes in biomass-bound EPS and Fe linked with EPS (Fe_{EPS}) in batches. (A) EPS polysaccharide. (B) EPS humic substances. (C) EPS protein. (D) Fe_{EPS}.

mechanisms other than photochemical reduction. Hence, the difference between bulk-liquid Fe(II) in light sets vs the dark control, especially during short periods like several hours of incubation, may serve as photogenerated Fe(II) (Figure 3B). It is clear that during the first day of batch incubation, the 450 μmol/m^2·s set led to the fastest and greatest release of Fe(II) into bulk liquids followed by 180 and 27 μmol/m^2·s sets. This strongly supports that greater light intensities led to greater extents of Fe reduction by the photoreduction pathway, i.e., ligand-to-metal charge transfer. When FZ was not added, the lowest level of bulk-liquid Fe was detected under 450 μmol/m^2·s (Figure 2). Hence, this result suggests that Fe(II) emanating from photoreduction is quickly available to phototrophs under illumination.[8,11] Fujii et al.[10] further supports the current discussion. In this study, cyanobacteria's Fe uptake rate significantly increased as the concentration of photogenerated unchelated Fe(II), from the Fe(III)-EDTA complex, increased. Notably, both photochemical release of Fe(II) and subsequent cyanobacterial uptake occurred primarily under the <500 nm spectrum of visible light, suggesting photochemical enhanced bioassimilation of Fe. Based on our results and findings from Fujii et al.,[10] we infer that unchelated Fe(II) from photochemical reduction is useful for cyanobacteria in photogranular cultivation because Gram-negative cyanobacteria can utilize porins, outer membrane transport proteins, to facilitate passive diffusion of Fe from environments,[58] whereas eukaryotic phototrophs have to use energy-demanding active transporters, which is also 10−1000 times slower than transport via porins.[10]

Nonetheless, greater Fe availability under higher light intensities, thus promoting faster phototrophic growth, would result in faster utilization of Fe, ultimately creating a faster Fe-limited environment. In this regard, it is worth noting that the speed of disappearance of $Fe^{II}FZ_3$ in batches was also proportional to light intensity (Figure 3A). These imply that generation of higher Fe-chelating powers, which led to dissociation of Fe from $Fe^{II}FZ_3$ and which is indicative of Fe-limited environments, also took place in the order of light intensity. Under 450 and 180 μmol/m^2·s, photogranules were formed in similar timing with and without FZ. Under 27 μmol/m^2·s with FZ, the photogranular formation was about a week faster than without FZ (data not shown).

Fate of Fe Linked with EPS (Fe_{EPS}) under Different Light Intensities. The above results indicate that there is a pool of Fe(III) in the solid phase of activated sludge, which is susceptible to photochemical reduction. The earlier hydrostatic batch study (PPFD of 18−45 μmol/m^2·s) with three different sources of activated sludge revealed that EPS proteins in activated sludge solids and Fe linked with EPS (Fe_{EPS}) became labile as photogranulation progressed.[32] The mass balance in the same study indicated that Fe_{EPS} in activated sludge inocula accounted for 3−8% of total Fe, while the intracellular Fe was also <10% of total Fe. These indicated that a significant amount of Fe in activated sludge is present as nonextractable Fe_{EPS} and Fe precipitates (predominantly ferric oxyhydroxides), which are much less likely available for microbial growth. Consequently, the study found that Fe_{EPS} and phycobilin strongly correlated, indicating that Fe_{EPS} is an important source of Fe for cyanobacteria. Importantly, spherical structures of photogranules appeared as the levels of Fe_{EPS} became steadily low, implying that the availability of Fe_{EPS} has a significant influence on cyanobacterial physiology and granulation. Thus, we aimed to examine the effect of light intensity on the fate of Fe_{EPS} and its relationship with the dynamics of bulk-liquid Fe and the speed of photogranulation observed under different light conditions (Figures 1 and 2).

Prior to analysis on Fe_{EPS}, we first checked how major organic fractions of EPS, polysaccharides, proteins, and humic

https://doi.org/10.1021/acs.est.3c00432
Environ. Sci. Technol. 2023, 57, 9086−9095

Table 1. Pearson Correlation Coefficients of Fe_{EPS} with Different Fractions of EPS and Photosynthetic Pigments of Biomass during the Hydrostatic Cultivation under Varying Light Intensities[b]

	dark control	27 μmol/m^2·s	180 μmol/m^2·s	450 μmol/m^2·s	450 μmol/m^2·s[a]
EPS-polysaccharide	0.67	−0.76	−0.26	0.44	−0.14
EPS-humic sub.	**0.87**	**0.93**	**0.89**	**0.91**	**0.93**
EPS-proteins	0.76	**0.90**	**0.85**	**0.83**	**0.82**
phycobilin	0.69	**−0.98**	**−0.86**	−0.29	**−0.88**
chlorophyll *a*	0.78	**−0.95**	**−0.89**	−0.58	**−0.84**
chlorophyll *b*	0.18	−0.78	**−0.89**	−0.58	**−0.84**
chlorophyll *c*	0.11	−0.74	−0.38	−0.13	**−0.87**

[a]Correlation coefficients for the data for the period of day 0 to day 9 only. [b]The bold numbers are indicated for $r > \pm 0.80$.

substances (EPS-PS, EPS-PN, and EPS-HU), changed under different light intensities. EPS-PS initially decreased by day 2 with the following increases in all light sets (Figure 4A). After day 2, the batch under 27 μmol/m^2·s showed a gradual increase to the highest point among the three light sets. An increase in EPS-PS in photogranule cultivation is indicative of the growth of motile filamentous cyanobacteria,[32,34] as they produce extracellular slime or mucilage for their motility.[59] Under 450 μmol/m^2·s, EPS-PS increased to day 8 but significantly decreased afterward, which concurs with the pattern of phycobilin (Figure 1B). Significant differences existed between the dark control and all light conditions for EPS-PS ($p < 0.002$). For EPS-PN and EPS-HU (Figure 4B,C), those that are nitrogenous organic-matter EPS, significant decreases over the course of all batches were obvious, indicating lability of these EPS pools during the hydrostatic batch of activated sludge regardless of light conditions. Yet, the results clearly illustrate that it was the 450 μmol/m^2·s set that led to the fastest and greatest declines in both EPS-HU and EPS-PN, indicating enhanced access and availability of these EPS fractions under strong light conditions.

The concentration of Fe present in the extracted EPS (Fe_{EPS}) was found to be on average 1.75 mg/L, 8.1% of total Fe in the inoculum. By the end of batch, the fraction of Fe_{EPS} decreased to 1.1−1.3% in the light sets compared to 4.4% in the dark control. A much larger amount of Fe_{EPS} remaining in the dark control suggests that this pool of Fe was not as available as in light batches. Congruent with the earlier study,[32] Fe_{EPS} (Figure 4D) showed similar patterns with EPS-HU and EPS-PN. Indeed, strong correlations were found between Fe_{EPS} and both EPS-HU and EPS-PN (Table 1), indicating that these nitrogenous EPS pools are the primary source of Fe_{EPS}. The results further suggest that, although extremely low levels of bulk-liquid Fe remained past its initial peak (from day 2 or 3, Figure 2), Fe from EPS-HU and EPS-PN was made available for significant durations of batches. Additionally, the early release of bulk-liquid Fe most likely originated from Fe_{EPS}, concurring with the results of +FZ batches (Figure 3A).

For decreases of Fe_{EPS} over batch periods, significant differences between light sets vs the dark control ($p < 0.009$ for the sets of 180 and 450 μmol/m^2·s; $p = 0.149$ for 27 μmol/m^2·s) again signify that Fe_{EPS} in activated sludge is susceptible to photochemical reactions absent in the dark control. In other words, a given fraction of Fe_{EPS} in activated sludge solids does not undergo reduction simply by the development of anaerobic conditions but is prone to photochemical reduction. Importantly, the rate of removal of this Fe pool in light batches followed the order of light intensity. Decreases of Fe_{EPS} for the first 12 days were well-described as second-order decays: the reaction rate constants k for 450, 180, and 27 μmol/m^2·s and the dark control were 0.26 ($R^2 = 0.94$), 0.13 ($R^2 = 0.94$), 0.06 ($R^2 = 0.95$), and 0.03 L/mg day ($R^2 = 0.81$), respectively. Faster dissociations of both Fe_{EPS} and nitrogenous EPS under 450 μmol/m^2·s suggest that EPS organic ligands complexed with Fe are good targets to photolysis, leading to the oxidation of EPS and reduction of Fe, under higher light intensities. Strong negative correlations between Fe_{EPS} and photosynthetic pigments (Table 1) suggest that this photolabile Fe became the source of phototrophic growth occurring in photogranule formation. Hence, stronger light and faster availability of Fe under such light conditions should have posed combined effects and led to faster phototrophic growth (Figure 1). This eventually causes faster limitation of Fe in batch systems, which of the period appears to correspond to the appearance of a granular morphology, suggesting physiological changes of microbes dealing with the limitation of essential nutrient Fe in the system. As mentioned above, under a high light intensity of 450 μmol/m^2·s, the established photogranule system also collapsed by losing cyanobacteria. Hence, the limited Fe under persistent high irradiation likely caused the eventual loss of cyanobacteria and granular integrity of photogranules.

Regardless of the rate of removal per light intensity, this Fe_{EPS} pool got eventually utilized in all light batches as it basically converged on the same lowest point. The slowest yet selective growth of cyanobacteria under 27 μmol/m^2·s and the slowest depletion of Fe_{EPS} in the same batch imply that a significant fraction of Fe_{EPS} was accessed by cyanobacteria during the photogranulation process. Under 27 μmol/m^2·s, Fe_{EPS} showed stronger correlations with phycobilin and chlorophyll *a* than chlorophyll *b* and chlorophyll *c* (Table 1), showing agreement of selection of cyanobacteria in this low-light cultivation set and their link with this Fe pool. On the other hand, correlations were similar for all measured pigments in 180 and 450 μmol/m^2·s sets, suggesting enrichment of both cyanobacteria and microalgae in photogranule formation under higher light sets. These results again suggest that the limitation of Fe_{EPS} has a strong influence on physiology of microbes, especially cyanobacteria, inducing the formation of granular aggregates.

IMPLICATIONS

This study presents that the photogranulation process is strongly influenced by light intensity, the availability of Fe, which is itself impacted by light intensity, and, thus, the combined effects of light and Fe. A greater light intensity enhances the speed of photogranulation not only by making more photons available for photosynthesis but also by accelerating the availability of Fe. Faster formation of photogranules under 450 μmol/m^2·s occurred with faster

https://doi.org/10.1021/acs.est.3c00432
Environ. Sci. Technol. 2023, 57, 9086−9095

photoreduction of Fe, in both liquid and solid phases of activated sludge, and faster depletion of bulk-liquid Fe and Fe_{EPS}. Slower yet still reaching the same lowest points of Fe_{EPS} in the two lower light sets and, importantly, the main granular structure appearing along with depletion of this particular pool of Fe in all three light sets strongly suggest that light and Fe cocontrol the photogranulation process.

For wastewater treatment, there is obvious interest in treating wastewater faster or in larger quantities. In this context, operating OPGs under high light intensities, thus achieving faster photogranulation, would be important. Furthermore, high light conditions are more relevant for OPG reactors operated under sunlight. This study suggests that it should be possible to pursue a "high-rate" OPG system under high light intensities, but it should be carefully approached due to the potential imbalance of light and Fe that it may bring.

Although photogranulation occurred faster under 450 μmol/m^2·s, this set also showed the loss of grown cyanobacteria and the rupture of the formed photogranules when batch was continued. This seems to make sense when considering the physiology of cyanobacteria, which has a high Fe requirement compared to other phototrophs and heterotrophic bacteria.[12,13] Under high light conditions with low Fe availability, cyanobacteria downregulate the biosynthesis of pigments and photosystems to avoid absorption of excess light energy. However, continued exposure to high-light/low-Fe conditions would lead to generating reactive oxygen species, causing photodamage to their cellular components.[1,60] In contrast, under low light conditions, cyanobacteria can grow and maintain with multiple Fe uptake mechanisms, including diffusive transport via porins and active transport involving siderophores,[61] and via enhanced phycobilin production.[60] Findings from Arcila and Buitrón,[62] who studied the effect of light intensity on a microalgae-bacterial system treating municipal wastewater in an 80 L high-rate algal pond, might be relevant to the current discussion. When this system was operated under high solar radiance (>1000 W/m^2), neither floc aggregation nor granulation was obtained but planktonic growth of green algae. However, when the light intensity was lowered to 479−665 W/m^2, with greenhouse nylon screens put on, the system ensued with bloom of filamentous cyanobacteria, which coincided with algal-bacterial granulation and effective treatment. These lines of literature and our observations suggest that to sustain OPG-based wastewater treatment under high light intensities, adequate reactor operating conditions should be implemented so that the loss of the cyanobacterial population can be avoided based on the imbalance in Fe and light levels.

In the earlier hydrostatic batch study in which the range of light intensity was 18−45 μmol/m^2·s, the main granular structure emerged as the Fe_{EPS} pool got depleted.[32] A very similar observation was also made from hydrodynamic batches, which occurred in a 1 L vessel with mixing and illumination at 126 μmol/m^2·s.[35] Per the current study, these observations apply to much higher light intensities. This study also showed that Fe_{EPS} in all batches became depleted along with the extensive growth of cyanobacteria, supported by strong correlations (Table 1). These observations tend to suggest that substantive growth of cyanobacteria on labile Fe (bulk-liquid Fe and Fe_{EPS}) and successive limitation of Fe induce granulation of cyanobacteria. This "feast−famine-like" nature may be relevant to the common use of a sequencing batch reactor (SBR) for granulation processes although the current hydrostatic batch does not involve repetitive feast−famine cycles as does the SBR.[31] This implies that reactors other than the SBR can be utilized to promote photogranulation if the feast−famine-like conditions can be induced. Indeed, we recently found that OPGs manifested in a 120 L continuous-flow completely stirred tank reactor (CSTR), which effectively treated organic matter in municipal wastewater in hydraulic retention of 6−24 h.[63,64] In this kind of situation, although no substrate gradient is expected to be present in the bulk liquid of the CSTR, it might be possible that different light and redox conditions developing along the depth of granules, especially in larger granules, induce a feast−famine pressure on Fe. This postulation seems to be supported by the observations made by Abouhend[65] that as the OPG biomass in SBR treating real wastewater grew in size (i.e., progression of granulation), both the concentration of Fe_{EPS} and its fraction in total Fe in the biomass substantially decreased.

This study thus reveals an important aspect of light/Fe coupling for photogranulation, a phenomenon that occurs across vastly different environments on our biosphere. For scale-up and sustaining OPGs in real continuous wastewater treatment, we propose that a better understanding of interactions of light and Fe and maintaining their balance by adequate reactor operations would be important. For the latter, we anticipate that various strategies including biomass wastage, biomass size control, scheme of mixing in deep reactors (dealing with both photoinhibition and photolimitation issues),[35,54] and/or the addition of Fe could be involved.

■ ASSOCIATED CONTENT

Supporting Information

The Supporting Information is available free of charge at https://pubs.acs.org/doi/10.1021/acs.est.3c00432.

Disintegration of the photogranular structure under high light incubation (Figure S1), microscopy of photogranules generated under three different light intensities (Figure S2), Fe(II) and Fe(III) in bulk liquids over the entire batch period (Figure S3), and changes in dissolved oxygen (Figure S4) (PDF)

■ AUTHOR INFORMATION

Corresponding Author

Chul Park − *Department of Civil and Environmental Engineering, University of Massachusetts, Amherst, Massachusetts 01003, United States;* orcid.org/0000-0003-0695-8562; Email: chulp@umass.edu

Authors

Abeera A. Ansari − *Department of Civil and Environmental Engineering, University of Massachusetts, Amherst, Massachusetts 01003, United States; U.S.-Pakistan Center for Advance Studies in Energy (USPCAS-E), National University of Sciences and Technology (NUST), Islamabad 44000, Pakistan*

Arfa A. Ansari − *Department of Civil and Environmental Engineering, University of Massachusetts, Amherst, Massachusetts 01003, United States*

Joseph G. Gikonyo − *Department of Civil and Environmental Engineering, University of Massachusetts, Amherst, Massachusetts 01003, United States;* orcid.org/0000-0001-5035-4059

https://doi.org/10.1021/acs.est.3c00432
Environ. Sci. Technol. 2023, 57, 9086−9095

Ahmed S. Abouhend − *Department of Civil and Environmental Engineering, University of Massachusetts, Amherst, Massachusetts 01003, United States;* orcid.org/0000-0002-0554-9495

Complete contact information is available at: https://pubs.acs.org/10.1021/acs.est.3c00432

Notes

The authors declare no competing financial interest.

■ ACKNOWLEDGMENTS

This work was supported by the grants from the National Science Foundation (IIP1919091), Massachusetts Clean Energy Center, the University of Massachusetts Amherst 2021 Manning/IALS Innovation Award, and the National University of Sciences and Technology, Pakistan.

■ REFERENCES

(1) Schoffman, H.; Lis, H.; Shaked, Y.; Keren, N. Iron−Nutrient Interactions within Phytoplankton. *Front. Plant Sci.* **2016**, *7*, 1223.
(2) Rochaix, J.-D. Regulation of Photosynthetic Electron Transport. *Biochim. Biophys. Acta, Bioenerg.* **2011**, *1807*, 375−383.
(3) Sandmann, G.; Malkin, R. Iron-Sulfur Centers and Activities of the Photosynthetic Electron Transport Chain in Iron-Deficient Cultures of the Blue-Green Alga Aphanocapsa. *Plant Physiol.* **1983**, *73*, 724−728.
(4) Raven, J. A.; Evans, M. C. W.; Korb, R. E. The Role of Trace Metals in Photosynthetic Electron Transport in O2-Evolving Organisms. *Photosynth. Res.* **1999**, *60*, 111−150.
(5) Rueter, J. G.; Petersen, R. R. Micronutrient Effects on Cyanobacterial Growth and Physiology. *N. Z. J. Mar. Freshw. Res.* **1987**, *21*, 435−445.
(6) Strzepek, R. F.; Harrison, P. J. Photosynthetic Architecture Differs in Coastal and Oceanic Diatoms. *Nature* **2004**, *431*, 689−692.
(7) Maldonado, M. T.; Price, N. M. Utilization of Iron Bound to Strong Organic Ligands by Plankton Communities in the Subarctic Pacific Ocean. *Deep Sea Res., Part II* **1999**, *46*, 2447−2473.
(8) Barbeau, K.; Rue, E. L.; Bruland, K. W.; Butler, A. Photochemical Cycling of Iron in the Surface Ocean Mediated by Microbial Iron(III)-Binding Ligands. *Nature* **2001**, *413*, 409−413.
(9) Faust, B. C.; Zepp, R. G. Photochemistry of Aqueous Iron(III)-Polycarboxylate Complexes: Roles in the Chemistry of Atmospheric and Surface Waters. *Environ. Sci. Technol.* **1993**, *27*, 2517−2522.
(10) Fujii, M.; Dang, T. C.; Rose, A. L.; Omura, T.; Waite, T. D. Effect of Light on Iron Uptake by the Freshwater Cyanobacterium Microcystis Aeruginosa. *Environ. Sci. Technol.* **2011**, *45*, 1391−1398.
(11) Maldonado, M. T.; Strzepek, R. F.; Sander, S.; Boyd, P. W. Acquisition of Iron Bound to Strong Organic Complexes, with Different Fe Binding Groups and Photochemical Reactivities, by Plankton Communities in Fe-Limited Subantarctic Waters. *Global Biogeochem. Cycles* **2005**, *19* (), DOI: 10.1029/2005GB002481.
(12) Lis, H.; Kranzler, C.; Keren, N.; Shaked, Y. A Comparative Study of Iron Uptake Rates and Mechanisms amongst Marine and Fresh Water Cyanobacteria: Prevalence of Reductive Iron Uptake. *Life Basel Switz.* **2015**, *5*, 841−860.
(13) Raven, J. A. Predictions of Mn and Fe Use Efficiencies of Phototrophic Growth as a Function of Light Availability for Growth and of C Assimilation Pathway. *New Phytol.* **1990**, *116*, 1−18.
(14) Sarmiento, J. L.; Hughes, T. M. C.; Stouffer, R. J.; Manabe, S. Simulated Response of the Ocean Carbon Cycle to Anthropogenic Climate Warming. *Nature* **1998**, *393*, 245−249.
(15) Brehm, U.; Krumbein, W. E.; Palińska, K. A. Microbial Spheres: A Novel Cyanobacterial−Diatom Symbiosis. *Naturwissenschaften* **2003**, *90*, 136−140.
(16) Malin, G.; Pearson, H. W. Aerobic Nitrogen Fixation in Aggregate-Forming Cultures of the Nonheterocystous Cyanobacterium Microcoleus Chthonoplastes. *Microbiology* **1988**, *134*, 1755−1763.
(17) Boedeker, C.; Immers, A. No More Lake Balls (Aegagropila Linnaei Kützing, Cladophorophyceae, Chlorophyta) in The Netherlands? *Aquat. Ecol.* **2009**, *43*, 891.
(18) Volkova, E.; Sorokovikova, E.; Belykh, O.; Tikhonova, I.; Bondarenko, N. Photogranules Formed by Filamentous Cyanobacteria and Algae of the Genus Spirogyra Link in the Coastal Zone of Lake Baikal. *Bull. Baikal State Univ.* **2020**, *30*, 14−22.
(19) Takeuchi, N.; Kohshima, S.; Seko, K. Structure, Formation, and Darkening Process of Albedo-Reducing Material (Cryoconite) on a Himalayan Glacier: A Granular Algal Mat Growing on the Glacier. *Arct. Antarct. Alp. Res.* **2001**, *33*, 115−122.
(20) Segawa, T.; Ishii, S.; Ohte, N.; Akiyoshi, A.; Yamada, A.; Maruyama, F.; Li, Z.; Hongoh, Y.; Takeuchi, N. The Nitrogen Cycle in Cryoconites: Naturally Occurring Nitrification-Denitrification Granules on a Glacier. *Environ. Microbiol.* **2014**, *16*, 3250−3262.
(21) Segawa, T.; Takeuchi, N.; Mori, H.; Rathnayake, R. M. L. D.; Li, Z.; Akiyoshi, A.; Satoh, H.; Ishii, S. Redox Stratification within Cryoconite Granules Influences the Nitrogen Cycle on Glaciers. *FEMS Microbiol. Ecol.* **2020**, *96*, fiaa199.
(22) Segawa, T.; Yonezawa, T.; Edwards, A.; Akiyoshi, A.; Tanaka, S.; Uetake, J.; Irvine-Fynn, T.; Fukui, K.; Li, Z.; Takeuchi, N. Biogeography of Cryoconite Forming Cyanobacteria on Polar and Asian Glaciers. *J. Biogeogr.* **2017**, *44*, 2849−2861.
(23) Takeuchi, N.; Sakaki, R.; Uetake, J.; Nagatsuka, N.; Shimada, R.; Niwano, M.; Aoki, T. Temporal Variations of Cryoconite Holes and Cryoconite Coverage on the Ablation Ice Surface of Qaanaaq Glacier in Northwest Greenland. *Ann. Glaciol.* **2018**, *59*, 21−30.
(24) Milferstedt, K.; Kuo-Dahab, W. C.; Butler, C. S.; Hamelin, J.; Abouhend, A. S.; Stauch-White, K.; McNair, A.; Watt, C.; Carbajal-González, B. I.; Dolan, S.; Park, C. The Importance of Filamentous Cyanobacteria in the Development of Oxygenic Photogranules. *Sci. Rep.* **2017**, *7*, 17944.
(25) Park, C.; Dolan, S. Algal-Sludge Granule for Wastewater Treatment and Bioenergy Feedstock Generation. US10189732B2, January 29, 2019. https://patents.google.com/patent/US10189732B2/en (accessed 2021-06-05).
(26) Trebuch, L. M.; Oyserman, B. O.; Janssen, M.; Wijffels, R. H.; Vet, L. E. M.; Fernandes, T. V. Impact of Hydraulic Retention Time on Community Assembly and Function of Photogranules for Wastewater Treatment. *Water Res.* **2020**, *173*, No. 115506.
(27) Trebuch, L. M.; Bourceau, O. M.; Vaessen, S. M. F.; Neu, T. R.; Janssen, M.; de Beer, D.; Vet, L. E. M.; Wijffels, R. H.; Fernandes, T. V. High Resolution Functional Analysis and Community Structure of Photogranules. *ISME J.* **2023**, 1−10.
(28) Ji, B.; Shi, Y.; Yılmaz, M. Microalgal-Bacterial Granular Sludge Process for Sustainable Municipal Wastewater Treatment: Simple Organics versus Complex Organics. *J. Water Process Eng.* **2022**, *46*, No. 102613.
(29) Abouhend, A. S.; McNair, A.; Kuo-Dahab, W. C.; Watt, C.; Butler, C. S.; Milferstedt, K.; Hamelin, J.; Seo, J.; Gikonyo, G. J.; El-Moselhy, K. M.; Park, C. The Oxygenic Photogranule Process for Aeration-Free Wastewater Treatment. *Environ. Sci. Technol.* **2018**, *52*, 3503−3511.
(30) Abouhend, A. S.; Milferstedt, K.; Hamelin, J.; Ansari, A. A.; Butler, C.; Carbajal-González, B. I.; Park, C. Growth Progression of Oxygenic Photogranules and Its Impact on Bioactivity for Aeration-Free Wastewater Treatment. *Environ. Sci. Technol.* **2020**, *54*, 486−496.
(31) Park, C.; Takeuchi, N. Unmasking Photogranulation in Decreasing Glacial Albedo and Net Autotrophic Wastewater Treatment. *Environ. Microbiol.* **2021**, *23*, 6391−6404.
(32) Ansari, A. A.; Ansari, A. A.; Abouhend, A. S.; Gikonyo, J. G.; Park, C. Photogranulation in a Hydrostatic Environment Occurs with Limitation of Iron. *Environ. Sci. Technol.* **2021**, *55*, 10672−10683.
(33) Stauch-White, K.; Srinivasan, V. N.; Camilla Kuo-Dahab, W.; Park, C.; Butler, C. S. The Role of Inorganic Nitrogen in Successful

Formation of Granular Biofilms for Wastewater Treatment That Support Cyanobacteria and Bacteria. *AMB Express* **2017**, *7*, 146.
(34) Kuo-Dahab, W. C.; Stauch-White, K.; Butler, C. S.; Gikonyo, G. J.; Carbajal-González, B.; Ivanova, A.; Dolan, S.; Park, C. Investigation of the Fate and Dynamics of Extracellular Polymeric Substances (EPS) during Sludge-Based Photogranulation under Hydrostatic Conditions. *Environ. Sci. Technol.* **2018**, *52*, 10462−10471.
(35) Gikonyo, J. G.; Ansari, A. A.; Abouhend, A. S.; Tobiason, J. E.; Park, C. Hydrodynamic Granulation of Oxygenic Photogranules. *Environ. Sci. Water Res. Technol.* **2021**, *7*, 427−440.
(36) Ansari, A. A.; Ansari, A. A.; Khoja, A. H.; Gikonyo, G. J.; Abouhend, A. S.; Park, C. The Fate and Dynamics of Iron during the Transformation of Activated Sludge into Oxygenic Photogranules (OPGs) under Hydrodynamic Batch Conditions for Environmental Applications. *J. Environ. Chem. Eng.* **2022**, *10*, No. 108190.
(37) Wang, D.; Li, A. Effect of Zero-Valent Iron and Granular Activated Carbon on Nutrient Removal and Community Assembly of Photogranules Treating Low-Strength Wastewater. *Sci. Total Environ.* **2022**, *806*, No. 151311.
(38) Gikonyo, J. G.; Ansari, A.; Park, C.; Tobiason, J. Physical Characterization of Oxygenic Photogranules. *Biochem. Eng. J.* **2022**, *186*, No. 108592.
(39) Smetana, G.; Grosser, A. The Oxygenic Photogranules—Current Progress on the Technology and Perspectives in Wastewater Treatment: A Review. *Energies* **2023**, *16*, 523.
(40) Pierson, B. K.; Parenteau, M. N.; Griffin, B. M. Phototrophs in High-Iron-Concentration Microbial Mats: Physiological Ecology of Phototrophs in an Iron-Depositing Hot Spring. *Appl. Environ. Microbiol.* **1999**, *65*, 5474−5483.
(41) Park, C.; Novak, J. T. Characterization of Activated Sludge Exocellular Polymers Using Several Cation-Associated Extraction Methods. *Water Res.* **2007**, *41*, 1679−1688.
(42) APHA. *Standard Methods for the Examination of Water and Wastewater*, 22nd ed.; American Public Health Association: Washington D.C., USA, 2012.
(43) Shaked, Y.; Kustka, A. B.; Morel, F. M. M. A General Kinetic Model for Iron Acquisition by Eukaryotic Phytoplankton. *Limnol. Oceanogr.* **2005**, *50*, 872−882.
(44) Shaked, Y.; Kustka, A. B.; Morel, F. M. M.; Erel, Y. Simultaneous Determination of Iron Reduction and Uptake by Phytoplankton. *Limnol. Oceanogr. Methods* **2004**, *2*, 137−145.
(45) Bennett, A.; Bogorad, L. Complementary Chromatic Adaptation in a Filamentous Blue-Green Alga. *J. Cell Biol.* **1973**, *58*, 419−435.
(46) Lauceri, R.; Bresciani, M.; Lami, A.; Morabito, G. Chlorophyll a Interference in Phycocyanin and Allophycocyanin Spectrophotometric Quantification. *J. Limnol.* **2018**, *77* (), DOI: 10.4081/jlimnol.2017.1691.
(47) DuBois, M.; Gilles, K. A.; Hamilton, J. K.; Rebers, P. A.; Smith, F. Colorimetric Method for Determination of Sugars and Related Substances. *Anal. Chem.* **1956**, *28*, 350−356.
(48) Frølund, B.; Griebe, T.; Nielsen, P. H. Enzymatic Activity in the Activated-Sludge Floc Matrix. *Appl. Microbiol. Biotechnol.* **1995**, *43*, 755−761.
(49) Lowry, O. H.; Rosebrough, N. J.; Farr, A. L.; Randall, R. J. Protein Measurement with the Folin Phenol Reagent. *J. Biol. Chem.* **1951**, *193*, 265−275.
(50) Ivanikova, N. Lake Superior Phototrophic Picoplankton: Nitrate Assimilation Measured with a Cyanobacterial Nitrate-Responsive Bioreporter and Genetic Diversity of the Natural Community. 2006, Ph.D. Dissertation, Bowling Green State University.
(51) Hunter, P. D.; Tyler, A. N.; Willby, N. J.; Gilvear, D. J. The Spatial Dynamics of Vertical Migration by Microcystis Aeruginosa in a Eutrophic Shallow Lake: A Case Study Using High Spatial Resolution Time-Series Airborne Remote Sensing. *Limnol. Oceanogr.* **2008**, *53*, 2391−2406.
(52) Nadeau, T.; Howard-Williams, C.; Castenholz, R. Effects of Solar UV and Visible Irradiance on Photosynthesis and Vertical Migration of Oscillatoria Sp. (Cyanobacteria) in an Antarctic Microbial Mat. *Aquat. Microb. Ecol.* **1999**, *20*, 231−243.
(53) Tilzer, M. M. Light-dependence of Photosynthesis and Growth in Cyanobacteria: Implications for Their Dominance in Eutrophic Lakes. *N. Z. J. Mar. Freshw. Res.* **1987**, *21*, 401−412.
(54) Gikonyo, J. G.; Keyser, A.; Tobiason, J.; Jeong, J.; Park, C. In Vivo Evaluation of Oxygenic Photogranules' Photosynthetic Capacity by Pulse Amplitude Modulation and Phototrophic−Irradiance Curves. *ACS EST Eng.* **2021**, *1*, 551−561.
(55) Melton, E. D.; Swanner, E. D.; Behrens, S.; Schmidt, C.; Kappler, A. The Interplay of Microbially Mediated and Abiotic Reactions in the Biogeochemical Fe Cycle. *Nat. Rev. Microbiol.* **2014**, *12*, 797−808.
(56) Schaedler, F.; Lockwood, C.; Lueder, U.; Glombitza, C.; Kappler, A.; Schmidt, C. Microbially Mediated Coupling of Fe and N Cycles by Nitrate-Reducing Fe(II)-Oxidizing Bacteria in Littoral Freshwater Sediments. *Appl. Environ. Microbiol.* **2018**, *84*, e02013−e02017.
(57) Wang, X.-M.; Waite, T. D. Iron Speciation and Iron Species Transformation in Activated Sludge Membrane Bioreactors. *Water Res.* **2010**, *44*, 3511−3521.
(58) Qiu, G.-W.; Koedooder, C.; Qiu, B.-S.; Shaked, Y.; Keren, N. Iron Transport in Cyanobacteria − from Molecules to Communities. *Trends Microbiol.* **2022**, *30*, 229−240.
(59) Hoiczyk, E. Gliding Motility in Cyanobacteria: Observations and Possible Explanations. *Arch. Microbiol.* **2000**, *174*, 11−17.
(60) Chakdar, H.; Pabbi, S. Cyanobacterial Phycobilins: Production, Purification, and Regulation. In *Frontier Discoveries and Innovations in Interdisciplinary Microbiology*; Shukla, P., Ed.; Springer India: New Delhi, 2016; pp. 45−69, DOI: 10.1007/978-81-322-2610-9_4.
(61) Rudolf, M.; Kranzler, C.; Lis, H.; Margulis, K.; Stevanovic, M.; Keren, N.; Schleiff, E. Multiple Modes of Iron Uptake by the Filamentous, Siderophore-Producing Cyanobacterium, Anabaena Sp. PCC 7120. *Mol. Microbiol.* **2015**, *97*, 577−588.
(62) Arcila, J. S.; Buitrón, G. Influence of Solar Irradiance Levels on the Formation of Microalgae-Bacteria Aggregates for Municipal Wastewater Treatment. *Algal Res.* **2017**, *27*, 190−197.
(63) Park, C.; Abouhend, A. S.; Gikonyo, J. G. System and Method for Cultivation of Oxygenic Photogranules. 2022. Provisional Patent Application 63/365,347.
(64) Gikonyo, J. G.; Abouhend, A. S.; Keyser, A.; Li, Y.; Park, C. Scaling-up of Oxygenic Photogranular System in Selective-CSTR. *Bioresource Technology Reports* (In revision).
(65) Abouhend, A. S. Size Progression of Oxygenic Photogranules (OPGs) and its Effect on OPG Wastewater Treatment. 2022, Ph.D. Dissertation, University of Massachusetts Amherst.

https://doi.org/10.1021/acs.est.3c00432
Environ. Sci. Technol. 2023, 57, 9086−9095